Biochemical Pharmacology 82 (2011) 236–247

Contents lists available at ScienceDirect

Biochemical Pharmacology

journal homepage: www.elsevier.com/locate/biochempharm

Effects of highly active novel artemisinin–chloroquinoline hybrid compounds on β-hematin formation, parasite morphology and endocytosis in *Plasmodium falciparum*

Tzu-Shean Feng [a,b], Eric M. Guantai [a,c], Margo Nell [d], Constance E.J. van Rensburg [d], Kanyile Ncokazi [a], Timothy J. Egan [a], Heinrich C. Hoppe [b,**], Kelly Chibale [a,e,*]

[a] *Department of Chemistry, University of Cape Town, Rondebosch 7701, South Africa*
[b] *Division of Pharmacology, University of Cape Town, Observatory 7925, South Africa*
[c] *Division of Pharmacology, School of Pharmacy, University of Nairobi, Box 19676-00202, Kenya*
[d] *Department of Pharmacology, University of Pretoria, Hatfield 0028, South Africa*
[e] *Institute of Infectious Disease and Molecular Medicine, University of Cape Town, Rondebosch 7701, South Africa*

ARTICLE INFO

Article history:
Received 5 April 2011
Accepted 29 April 2011
Available online 8 May 2011

Keywords:
Artemisinin
β-Hematin inhibition
Chloroquinoline
Endocytosis
Parasite morphology
Plasmodium falciparum

ABSTRACT

4-Aminoquinolines were hybridized with artemisinin and 1,4-naphthoquinone derivatives via the Ugi-four-component condensation reaction, and their biological activities investigated. The artemisinin-containing compounds **6a–c** and its salt **6c-citrate** were the most active target compounds in the antiplasmodial assays. However, despite the potent *in vitro* activities, they also displayed cytotoxicity against a mammalian cell-line, and had lower therapeutic indices than chloroquine. Morphological changes in parasites treated with these artemisinin-containing hybrid compounds were similar to those observed after addition of artemisinin. These hybrid compounds appeared to share mechanism(s) of action with both chloroquine and artemisinin: they exhibited potent β-hematin inhibitory activities; they caused an increase in accumulation of hemoglobin within the parasites that was intermediate between the increase observed with artesunate and chloroquine; and they also appeared to inhibit endocytosis as suggested by the decrease in the number of transport vesicles in the parasites. No cross-resistance with chloroquine was observed for these hybrid compounds, despite the fact that they contained the chloroquinoline moiety. The hybridization strategy therefore appeared to be borrowing the best from both classes of antimalarials.

1. Introduction

Malaria remains one of the most widespread infectious diseases and poses a great challenge to world health. Over 200 million episodes of malaria occur annually, occasioning approximately 1 million deaths every year, mainly among children and pregnant women in sub-Saharan Africa [1–4]. Resistance of malaria parasites to available antimalarial drugs remains the main challenge to the effective control of the disease. *Plasmodium falciparum* is the predominant *Plasmodium* species in Africa, the most virulent species of the malaria parasite and the cause of the bulk of the mortality associated with malaria. Over the last half a century this species has developed significant degrees of resistance to many classes of drugs [3,5,6]. Of particular concern is the recent evidence of the possible emergence of resistance to artemisinin-based antimalarials in Southeast Asia, a situation that could threaten the current clinical efficacy of the first-line artemisinin-combination therapy (ACT) strategies [7,8].

This has led to extensive drug discovery efforts aimed at developing novel antimalarial compounds or modifying existing agents in the hope of identifying new, highly efficacious drugs to supplement available drugs for the treatment of malaria [9]. As part of these efforts, we undertook to synthesize a variety of hybrid compounds combining features of artemisinin, 1,4-naphthoquinone and chloroquine for biological investigation. Artemisinins and chloroquine are established antimalarial drugs, and their antimalarial activities have been extensively studied and exploited both experimentally and clinically [10–12]. In addition, the precedent already exists for the fusion of artemisinin and aminoquinoline components to yield highly potent hybrid compounds [13,14].

* Corresponding author at: Department of Chemistry, University of Cape Town, Rondebosch 7701, South Africa. Tel.: +27 21 650 2553; fax: +27 21 650 5195.
** Corresponding author. Tel.: +27 12 841 4363; fax: +27 12 841 4790.
E-mail addresses: HHoppe@csir.co.za (H.C. Hoppe), Kelly.Chibale@uct.ac.za (K. Chibale).

0006-2952/$ – see front matter © 2011 Elsevier Inc. All rights reserved.
doi:10.1016/j.bcp.2011.04.018

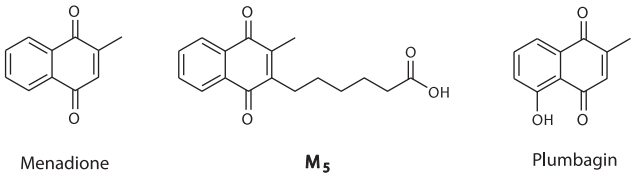

Fig. 1. Examples of 1,4-naphthaquinone inhibitors of glutathione reductase.

1,4-Naphthoquinones, on the other hand, are an important class of inhibitors of glutathione (and thioredoxin) reductase, with plumbagin, menadione and its hexanoic acid derivative **M_5** being representative examples (Fig. 1) [15,16]. Glutathione reductase is the enzyme responsible for regenerating the reduced form of glutathione, a major (di)thiol responsible for the prevention of oxidative damage in both human cells and the malaria parasite by the detoxification of reactive oxygen radicals [17]. Glutathione has also been suggested to be involved in the degradation of toxic heme formed by the malaria parasite during hemoglobin digestion [17], though the main route of detoxification has been shown to be mainly via the conversion of heme to hemozoin (malaria pigment), an inert, crystalline form of heme [18,19]. Double headed prodrugs and other hybrid compounds based on 1,4-naphthoquinones and 4-aminoquinolines have previously been developed and proven to be potent antimalarials *in vitro* and *in vivo*, exerting their effects by inhibiting glutathione reductase [16,20,21].

1,4-Naphthoquinone and artemisinin were therefore chosen for hybridization to 4-aminoquinolines to afford the target hybrid compounds **6a–e** (Fig. 3), using the Ugi four-component condensation (Ugi-4CC) reaction [22] as the hybridization strategy. This reaction is an example of a multi-component reaction (MCR), i.e. chemical reactions that utilize three or more different starting materials as chemical inputs in a one-step-one-pot synthesis to yield one single product that contains features of all inputs. Such reactions are highly efficient as they create molecular complexity by generating more than two chemical bonds per operation, and are widely used to study structure-activity relationships and also to create libraries of organic molecules [23]. The Ugi-4CC utilizes an aldehyde, an amine, an acid and an isocyanide, and converts them into an α-acetamidoamide in one step and usually in good yields.

Based on its versatility, the Ugi-4CC was selected as the chemical approach for the synthesis of the target hybrid compounds combining features of artemisinin, 1,4-naphthoquinone and chloroquine (Fig. 2). The synthesis and results from the biological evaluation of the target compounds are reported herein.

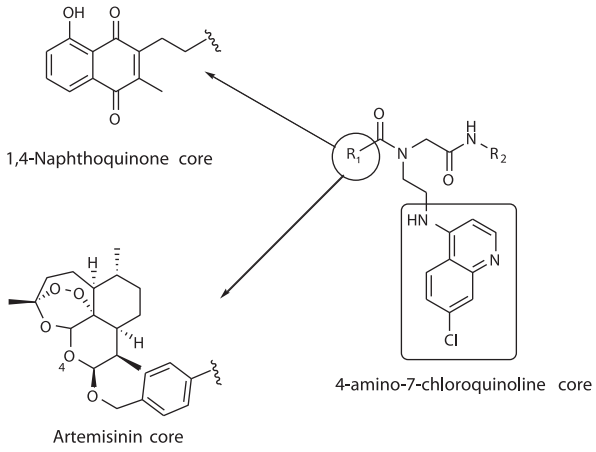

Fig. 2. General structure showing the design of the target compounds.

Fig. 3 shows the chemical structures of the target hybrid compounds **6a–e**.

Following their synthesis, the target compounds were assessed for their biological activities, including *in vitro* antiplasmodial activity, inhibition of β-hematin formation, effects on parasite morphology, and effects on hemoglobin endocytosis by the parasite. The latter experiments were motivated by the reported differential activities of quinolines and artemisinin on endocytosis and endocytic trafficking in malaria parasites [24]. Chloroquine is thought to interfere with the parasite endocytic pathway by blocking the fusion of hemoglobin transport vesicles to the digestive food vacuole, resulting in an accumulation of undigested hemoglobin in transport vesicles. By contrast, artemisinin does not inhibit transport vesicle-vacuole fusion, but rather the preceding endocytosis of hemoglobin and formation of the transport vesicles, while there are additional indications of an inhibition of the proteolytic digestion of hemoglobin inside the food vacuole [24]. The biological effects of the test compounds were used to obtain a preliminary indication of their modes of action vis-à-vis chloroquine and artemisinin.

2. Materials and methods

Chemicals and reagents were purchased from either Sigma-Aldrich or Merck, South Africa. Chromatography solvents were purchased from Kimix Chemicals or Protea Chemicals, South Africa, as Chemically Pure (CP grade) solvents and distilled before use.

2.1. Chemistry

The Ugi-4CC utilizes an acid, an amine, an aldehyde and an isocyanide, and converts them into an α-acetamidoamide in one step. The target Ugi adducts were synthesized using either artelinic acid **2** or 1,4-naphthoquinone-acid **3** as the acid component; either of the 4-aminoquinoline amines **4** or **5** as the amine component; paraformaldehyde as the aldehyde input; and cyclohexyl- and *tert*-butyl isocyanide as the isocyanide component (Scheme 1).

2.1.1. Methyl p-[(10-dihydroartemisininoxy)methyl]benzoate (1)

Dihydroartemisinin (1.00 g, 3.500 mmol, 1.0 eq) and 4-(hydroxylmethyl)-benzoate (2.036 g, 12.006 mmol, 3.43 eq) were stirred in anhydrous Et_2O under N_2, where $BF_3{\cdot}Et_2O$ (0.50 ml, 3.955 mmol, 1.13 eq) was added drop-wise. The solution was stirred under N_2 at room temperature for 23 h, washed with 5% $NaHCO_3$ (until pH 8), H_2O (2 × 100 ml), dried (Na_2SO_4) and solvent evaporated. The crude product was purified via column chromatography (EtOAc/Hex, 1:9) to yield the pure product **1** as colourless oil (1.460 g, 97% (both α- and β-isomers)). R*f* (EtOAc/Hex 1:9) 0.21. β-Isomer: δ_H (400 MHz; $CDCl_3$) 8.01 (d, *J* 8.4, 2H, H19), 7.37 (d, *J* 8.4, 2H, H18), 5.44 (s, 1H, H12), 4.95 (d, *J* 13.2, 1H, H17), 4.91 (d, *J* 3.2, 1H, H10), 4.57 (d, *J* 13.2, 1H, H17), 3.91 (s, 3H, OCH_3), 2.69 (m, 1H, H9), 2.36 (ddd, *J* 14.0, 13.2 and 4.0, 1H, not known[1]), 2.20–1.50 (m, 4H, not known[1]), 1.45 (s, 3H, H14), 0.96 (d, *J* 7.6, 3H, H15), 0.94 (d, *J* 6.4, 3H, H16). α-Isomer: δ_H (400 MHz; $CDCl_3$) 8.00 (d, *J* 8.4, 2H, H19), 7.43 (d, *J* 8.8, 2H, H18), 5.34 (s, 1H, H12), 5.02 (d, *J* 14.2, 1H, H17), 4.68 (d, *J* 13.2, 1H, H17), 4.52 (d, *J* 9.2, 1H, H10), 3.91 (s, 3H, OCH_3), 2.53 (m, 1H, H9), 2.39 (ddd, *J* 14.4, 13.2 and 4.0, 1H, not known[1]), 2.20–1.50 (m, 4H, not known[1]), 1.45 (s, 3H, H14), 0.93 (d, *J* 5.6, 3H, H16), 0.93 (d, *J* 7.2, 3H, H15).

2.1.2. 2.1.2 p-[(10-Dihydroartemisininoxy)methyl]benzoic acid (Artelinic Acid) (2)

The methyl ether **1** (1.272 g, 2.932 mmol) was stirred in 2.5% KOH/MeOH (25 ml) at room temperature for 3 days, and the solvent removed under reduced pressure. The residue was

[1] Protons could not be assigned due to complexity.

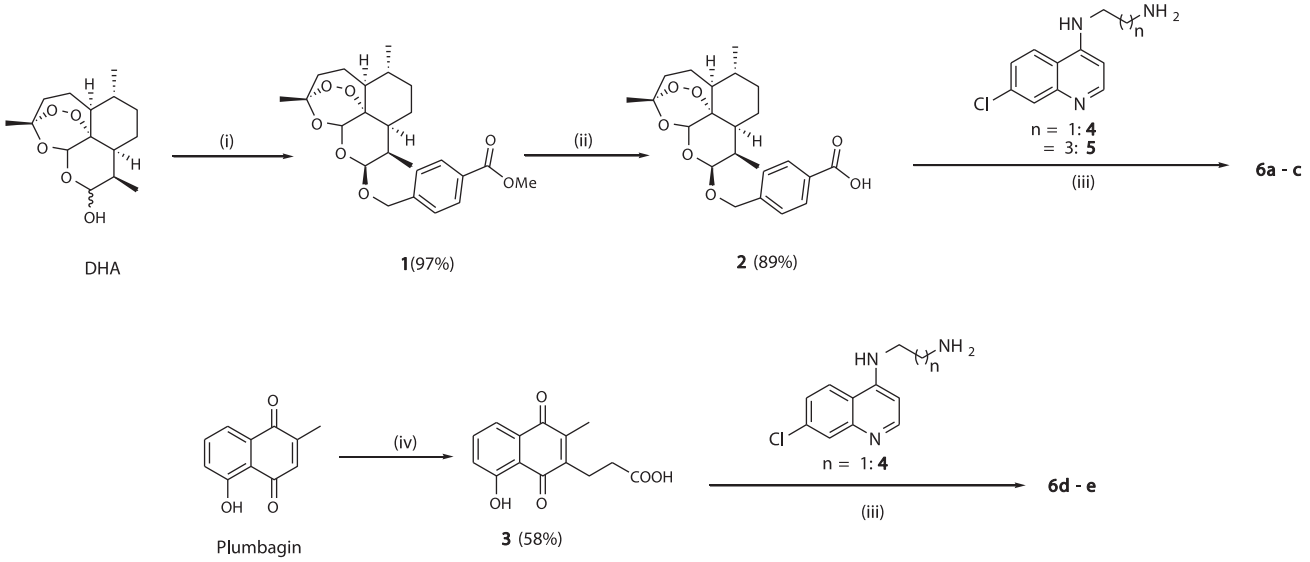

Scheme 1. *Reagents and conditions*: (i) methyl 4-(hydroxymethyl)-benzoate (3.4 eq), $BF_3{\cdot}Et_3O$ (1.13 eq), Et_3O, N_2, r.t., 24 h; (ii) 2.5% KOH/MeOH, r.t., 3 days; (iii) succinic acid (3.0 eq), silver nitrate (0.5 eq), ammonium persulfate (1.3eq), 30% aq. CH_3N, 65–70 °C, 3 h.; (iv) **2** or **3** (1.0 eq), amine **4** or **5** (1.2 eq), aldehyde (1.0 eq), cyclohexyl- or *tert*-butyl isocyanide (1.0 eq), MeOH, r.t., 3–5 days.

dissolved in H_2O (25 ml), and the pH adjusted to 8 via addition of acetic acid. The solution was extracted with Et_2O (3 × 50 ml), dried (Na_2SO_4) and solvent evaporated. The resulting oil was seeded and the pure compound crystallized out to yield white crystals (1.091 g, 89%). m.p. 141–144 °C (lit. 142–145 °C) [25]. R*f* (EtOAc/Hex 3.3:6.7) 0.18. β-Isomer: δ_H (300 MHz; $CDCl_3$) 8.01 (d, *J* 8.4, 2H, H19), 7.40 (d, *J* 8.4, 2H, H18), 5.45 (s, 1H, H12), 4.98 (d, *J* 13.5, 1H, H17), 4.93 (d, *J* 3.0, 1H, H10), 4.60 (d, *J* 13.5, 1H, H17), 2.70 (m, 1H, H9), 2.38 (ddd, *J* 14.0, 13.2 and 4.0, 1H, not known[1]), 2.20–1.50 (m, 4H, not known[1]), 1.45 (s, 3H, H14), 0.98 (d, *J* 7.2, 3H, H15), 0.95 (d, *J* 6.0, 3H, H16). α-Isomer: δ_H (300 MHz; $CDCl_3$) 8.06 (d, *J* 8.4, 2H, H19), 7.46 (d, *J* 8.4, 2H, H18), 5.35 (s, 1H, H12), 5.05 (d, *J* 13.5, 1H, H17), 4.70 (d, *J* 13.2, 1H, H17), 4.53 (d, *J* 9.0, 1H, H10), 2.55 (m, 1H, H9), 2.39 (ddd, *J* 14.4, 13.2 and 4.2, 1H, not known[1]), 2.20–1.50 (m, 4H, not known[1]), 1.46 (s, 3H, H14), 0.95 (d, *J* 6.0, 3H, H16), 0.94 (d, *J* 7.2, 3H, H15).

The β-isomer was the major product (diastereomeric ratio α:β 2:98) as confirmed by the integrations on ^{1}H NMR spectroscopy.

2.1.3. 2.1.3 3-Carboxyethyl-5-hydroxy-2-methyl-1,4-naphthoquinone (3)

Plumbagin (1.00 g, 5.314 mmol, 1.0 eq) and succinic acid (1.902 g, 15.942 mmol, 3.0 eq) were stirred in 30% aqueous acetonitrile (40 ml) at 65 °C, followed by the addition of silver nitrate (0.456 g, 2.657 mmol, 0.5 eq). A solution of ammonium persulfate (1.609 g, 6.908 mmol, 1.3 eq) in 30% aqueous acetonitrile (20 ml) was added drop-wise over 2 h, and the resulting solution stirred at 65–70 °C for 3 h. On cooling, the mixture was extracted with EtOAc (4 × 60 ml), and the organic layer washed with H_2O (3 × 20 ml), dried (Na_2SO_4) and solvent evaporated. The crude material was purified via column chromatography (DCM/MeOH 9.5:0.5) to yield the pure product as an orange powder (0.581 g, 58%). m.p. 155–159 °C [26]. R*f* (CH_2Cl_2/MeOH, 9.5:0.5) 0.49. δ_H (400 MHz; $CDCl_3$) 7.62 (d, *J* 6.8, 1H, H8), 7.57 (t, *J* 7.6, 1H, H7), 7.23 (d, *J* 7.6, H6), 2.98 (t, *J* 7.6, 2H, H11), 2.62 (t, *J* 7.6, 2H, H10), 2.23 (s, 3H, CH_3).

2.1.4. General method A for the preparation of 4 and 5

Et_3N (0.3 eq) was added drop-wise to a stirred solution of 4,7-dichloroquinoline (1.0 eq) and K_2CO_3 (0.5 eq) in respective diamines (20.0 eq) and refluxed at 110 °C for 4 h. Products that precipitated on cooling were filtered and washed with brine and H_2O. For products that stayed in solution, NaOH was added, and the organic product was immediately basified with 10% NaOH (w/v) and extracted with EtOAc (5 times), washed with H_2O (2 times) and dried (Na_2SO_4). Recrystallization from EtOAc afforded the amine in excellent yields.

2.1.5. N-(7-Chloroquinolin-4-yl)-ethane-1,2-diamine (4)

Pure product was recrystallized from EtOAc as white powder (0.4861 g, 64%). m.p. 136–138 °C (lit. 137–139 °C) [27]. R*f* (MeOH/CH_2Cl_2, 0.5:9.5) 0.32. δ_H (400 MHz; DMSO-*d6*) 8.38 (d, *J* 5.6, 1H, H2), 8.10 (d, *J* 8.4 Hz, 1H, H5), 7.76 (d, *J* 2.0, 1H, H8), 7.40 (dd, *J* 8.4 and 2.0, 1H, H6), 7.24 (br s, 1H, NH), 6.48 (d, *J* 5.6, 1H, H3), 3.25 (t, *J* 5.6, 2H, H9), 2.82 (t, *J* 6.0, 2H, H10).

2.1.6. N-(7-Chloroquinolin-4-yl)-butane-1,4-diamine (5)

Pure product was recrystallized from EtOAc as a light-yellow solid (1.60 g, 87%). m.p. 43–46 °C (lit. 43–47 °C) [27]. R*f* (NH_3/MeOH, 1:49) 0.22. δ_H (300 MHz; CD_3OD) 8.48 (d, *J* 5.7, 1H, H2), 7.96 (d, *J* 9.0 Hz, 1H, H5), 7.69 (d, *J* 2.1, 1H, H8), 7.27 (dd, *J* 9.0 and 2.1, 1H, H6), 6.34 (d, *J* 5.7, 1H, H3), 3.40 (t, *J* 7.2, 2H, H9), 3.04 (t, *J* 7.2, 2H, H12), 1.88 (m, 2H, H10), 1.62 (m, 2H, H11).

2.1.7. Ugi adduct (6a)

Purified via column chromatography, first with EtOAC and then with EtOAC/MeOH 9.5:0.5 to yield the pure product as a white powder (0.5115 g, 89%). (m.p. 121–124 °C. R*f* (MeOH/EtOAC, 1:9) 0.18; ν_{max} ($CHCl_3$)/cm^{-1} 3223 (N–H), 2920 (Ar–H), 1580 (C=O), 1216 (C–N), 781 (C–Cl); δ_H (400 MHz; $CDCl_3$) 8.45 (br s, 1H, H24), 8.28 (br s, 1H, H26), 7.96 (br s, 2H, H19), 7.41 (d, *J* 8.8, 2H, H18), 7.39 (br s, 1H, H27), 7.03 (br s, 1H, H27), 6.35 (br s, 1H, H25), 5.42 (s, 1H, H12), 4.88 (br s, 2H, H17 + H10), 4.51 (br s, 1H, H17), 4.09 (m, 2H, H22), 3.61 (br s, 2H, H23), 2.68 (m, 1H, H9), 2.38 (ddd, *J* 14.4 and 13.2, 4.2 Hz, 1H, not known), 1.45–1.93 (m, 15H), 1.44 (s, 3H, H14), 0.95 (d, *J* 6.0, 6H, H16 + H15); δ_c (75.5 MHz; DMSO-*d6*) 171.6, 171.0, 170.2, 167.5, 151.9, 151.5, 150.1, 149.5, 149.1, 139.9, 139.2, 135.2, 134.9, 133.4, 127.5, 126.6, 126.3, 124.1, 123.7, 123.5, 117.5, 103.3, 100.6, 98.6, 87.0, 80.4, 52.0, 47.7, 36., 34.0, 32.1, 30.5, 25.6, 25.1, 24.4, 24.2, 20.0, 12.7; (Found: *m*/*z*, 761.3596 [M+], $C_{42}H_{53}ClN_4O_7$ requires *M*, 761.3584) (Found: C, 66.00, H, 7.26, N, 7.67%; Requires C, 66.26, H, 7.02 N, 7.36%).

*2.1.8. Ugi adduct (**6b**)*

Purified via column chromatography, first with EtOAc and then with EtOAc/MeOH 9.5:0.5 to yield the pure product as a white powder (0.5009 g, 84%). (m.p. 121–123 °C. R*f* (MeOH/EtOAc, 1:9) 0.48; ν_{max} ($CHCl_3$)/cm^{-1} 3333 (N–H), 2926 (Ar–H), 2894 (alkyls), 1666 (C=O), 1580 (Ar–C), 1010 (C–N), 753 (C–Cl); δ_H (400 MHz; $CDCl_3$) 8.45 (d, *J* 5.2, 1H, H24), 8.23 (br s, 1H, H29), 7.99 (s, 2H, H31), 7.36 (br s, 5H, H30 + H18 + H19), 7.13 (br s, 1H, NH), 6.31 (br s, 1H, H28), 6.10 (br s, 1H, NH), 5.44 (s, 1H, H12), 4.91 (d, *J* 12.4, 1H, H17), 4.90 (d, *J* 4.0, 1H, H10), 4.56 (d, *J* 12.4, 1H, H17), 4.11 (m, 2H, CH_2, H22), 3.81 (br s, 2H, CH_2, H25), 3.52 (br s, 2H, CH_2, H23), 3.48 (s, 2H, H20), 3.26 (br s, 2H, CH_2, H24), 2.52 (m, 1H, H9), 2.00–1.45 (m, 20H), 1.45 (s, 3H, H14), 0.96 (d, *J* 7.2, 3H, H15), 0.95 (d, *J* 5.6, 3H, H16); δ_c (100 MHz; DMSO-*d6*) 170.9, 167.1, 151.8, 150.0, 149.0, 139.5, 135.7, 132.3, 127.4, 126.8, 126.6, 126.5, 124.4, 124.0, 123.9, 117.4, 103.3, 100.6, 98.6, 87.0, 80.4, 68.7, 52.0, 47.6, 45.8, 43.7, 42.3, 36.6, 36.0, 34., 32.4, 32.1, 30.5, 25.6, 24.7, 24.4, 20.0, 12.7; (Found: *m*/*z* 789.4125 [M+], $C_{44}H_{57}ClN_4O_7$ requires *M*, 789.4122) (Found: C, 66.80, H, 6.91, N, 6.92%; Requires C, 66.95, H, 7.28 N, 7.10%).

*2.1.9. Ugi adduct (**6c**)*

Purified via column chromatography, first with EtOAc and then with EtOAc/MeOH 9.5:0.5 to yield the pure product as a white powder (0.453 g, 82%). (m.p. 127–129 °C. R*f* (MeOH/EtOAc, 1:9) 0.18; ν_{max} ($CHCl_3$)/cm^{-1} 3385 (N–H), 3017 (Ar–H), 1520 (C=O), 1215 (C–N), 756 (C–Cl); δ_H (400 MHz; $CDCl_3$) 8.47 (br s, 1H, H24), 8.24 (br s, 1H, H26), 8.12 (d, *J* 8.6, 2H, H19), 8.00 (s, 1H, H28), 7.40 (d, *J* 8.6, 2H, H18), 7.39 (br s, 1H, H27), 7.04 (br s, 1H, NH), 6.35 (br s, 1H, H25), 5.42 (s, 1H, H12), 4.87 (br s, 2H, H17 + H10), 4.51 (br s, 1H, H17), 3.93 (br s, 2H, H22), 3.64 (br s, 2H, H23), 2.68 (m, 1H, H9), 2.38 (ddd, *J* 14.4, 13.2 and 4.2, 1H, not known), 2.10–1.57 (m, 4H), 1.44 (s, 3H, H14), 1.35 (s, 9H, *t*-butyl), 0.95 (d, *J* 6.0, 6H, H16 + H15); δ_c (100 MHz; $CDCl_3$) 129.9, 127.2, 126.8, 125.9, 104.2, 104.2, 101.6, 101.6, 98.2, 88.1, 81.1, 70.7, 69.5, 69.1, 52.7, 52.6, 52.1, 44.5, 44.4, 37.5, 36.4, 34.6, 31.0, 30.9, 29.1, 28.7, 26.2, 24.7, 24.6, 20.3, 13.1; (Found: *m*/*z* 735.3211 [M+], $C_{40}H_{51}ClN_4O_7$ requires *M*, 735.3205) (Found: C, 65.68, H, 7.28, N, 7.56%; Requires C, 65.34, H, 6.99 N, 7.62%).

*2.1.10. Citrate salt of Ugi adduct **6c** (**6c-citrate**)*

Citric acid (0.131 g, 0.680 mmol, 2.5 eq) in acetone (5 ml) was added to a solution of **6c** (0.200 g, 0.272 mmol, 1.0 eq) in acetone (5 ml). The product precipitated out over 2 days at 4 °C to yield white solid (0.247 g, 98%). ν_{max} ($CHCl_3$)/cm^{-1} 3419 (OH (alcohol)), 3317 (N–H), 3017 (Ar–H), 2962 (OH (acid)), 1707 (C=O), 1612 (Ar–H), 1215 (C–N), 1007 (C–O), 752 (C–Cl); δ_H (300 MHz; CD_3OD) 8.51 (br s, 1H, H24), 8.43 (br s, 1H, H26), 7.91 (br s, 1H, H28), 7.61 (br s, 1H, H27), 7.39 (br s, 2H, H19), 6.99 (br s, 2H, H18), 6.42 (br s, 1H, H25), 5.44 (s, 1H, H12), 4.04 (br s, 2H, H22), 3.95 (br s, 2H, H23), 2.58 (m, 1H, H9), 2.33 (td, *J* 14.4 and 13.0, 4.2 Hz, 1H, not known), 2.20–1.50 (m, 4H, not known), 1.44 (br s, 4H, H29 + H30), 1.37 (s, 3H, H14), 1.32 (s, 9H, *t*-butyl), 0.94 (d, *J* 6.0, 6H, H16 + H15); (Found:, *m*/*z* 927.4471 [M+], $C_{40}H_{51}N_4ClO_7$ requires *M*, 927.4459) (Found: C, 59.76, H, 6.63, N, 5.74%; Requires C, 59.57, H, 6.41, N, 6.04%).

*2.1.11. N-(2-(7-Chloroquinolin-4-ylamino)ethyl)-N-(2-(cyclohexylamino)-2-oxoethyl)-3-(3-methyl-1,4-dioxo-1,4-dihydronaphthalen-2-yl)propanamide (**6d**)*

Purified via column chromatography, first with EtOAc and then with EtOAc/MeOH 9.5:0.5 to yield the pure product as an orange powder (0.1138 g, 25%). (m.p. 135–138 °C. R*f* (MeOH/EtOAc, 1:9) 0.11; ν_{max} ($CHCl_3$)/cm^{-1} 3273 (N–H), 3020 (Ar–H), 2926 (alkyls), 1606 (C=O), 1430 (Ar–C), 1216 (C–N), 770 (C–Cl); δ_H (300 MHz; $CDCl_3$) 8.48 (d, *J* 5.7, 1H, H10), 8.44 (d, *J* 5.4, 1H, H10), 7.96 (d, *J* 1.8, 1H, H14), 7.88 (d, *J* 1.8, 1H, H14), 7.88 (d, *J* 9.0, 1H, H12), 7.74 (d, *J* 9.0, 1H, H12), 7.55 (m, 4H, (H2 + H3) × 2), 7.35 (dd, *J* 9.0 and 1.8, 1H, H13), 7.31 (dd, *J* 9.0 and 1.8, 1H, H13), 7.13 (d, *J* 7.5, 1H, H1), 7.13 (d, *J* 7.5, 1H, H1), 6.97 (br s, 1H, NH), 6.34 (d, *J* 5.4, 1H, H11), 6.33 (d, *J* 5.7, 1H, H11), 4.09 (s, 2H, H7),4.00 (s, 2H, H7), 3.88 (m, 2H, H8), 3.70 (br s, 4H, H8 + H9), 3.50 (m, 2H, H9), 2.97 (t, *J* 7.8, 2H, H6), 2.72 (t, *J* 8.1, 2H, H5), 2.57 (t, *J* 7.8, 2H, H6), 2.28 (t, *J* 8.1, 2H, H5), 2.24 (s, 3H, H4), 1.92 (s, 3H, H4), 1.75 (m, 11H, cyclohexyl-H), 1.22 (m, 11H, cyclohexyl-H); δ_c (100 MHz; $CDCl_3$) 174.9, 161.2, 151.6, 151.0, 137.3, 136.8, 136.2, 136.1, 132.0, 125.9, 125.8, 125.7, 123.9, 122.2, 122.0, 119.2, 119.1, 98.6, 98.0, 53.1, 43.0, 41.0, 32.9, 32.2, 31.5, 25.5, 25.2, 24.8, 24.7, 22.7, 22.4, 12.9; (Found: *m*/*z* 603.1182 [M+], $C_{33}H_{35}ClN_4O_5$ requires *M*, 603.1177) (Found: C, 66.67, H, 7.07, N, 7.29%; Requires C, 66.95, H, 7.28 N, 7.10%).

2.1.12. N-(2-(tert-Butylamino)-2-oxoethyl)-N-(2-(7-chloroquinolin-4-ylamino)ethyl)-3-(3-methyl-1,4-dioxo-1,4-dihydronaphthalen-2-yl)propanamide (6e)

Purified via column chromatography, first with EtOAc and then with EtOAc/MeOH 9.5:0.5 to yield the pure product as an orange powder (0.123 g, 28%). m.p. 205–207 °C; R*f* (EtOAc) 0.11; ν_{max} ($CHCl_3$)/cm^{-1} 3320 (N–H), 3026 (Ar–H), 1736 (C=O), 1430 (Ar–C), 1216 (C–N); 753 (C–Cl); δ_H (400 MHz; $CDCl_3$) 8.35 (d, *J* 5.2, 1H, H10), 8.34 (d, *J* 5.2, 1H, H10), 7.90 (d, *J* 9.2, 1H, H12), 7.85 (d, *J* 2.0, 1H, H14), 7.84 (d, *J* 9.2, 1H, H12), 7.79 (d, *J* 2.0, 1H, H14), 7.51 (m, 4H, (H2 + H3) × 2), 7.29 (dd, *J* 9.2 and 2.0, 1H, H13), 7.28 (dd, *J* 9.2 and 2.0, 1H, H13), 7.15 (d, *J* 7.2, 1H, H1), 7.14 (d, *J* 7.2, 1H, H1), 6.36 (d, *J* 5.6, 1H, H11), 6.35 (d, *J* 5.6, 1H, H11), 3.99 (s, 2H, H7), 3.79 (s, 2H, H7), 3.77 (d, *J* 5.6, 2H, H8), 3.66 (d, *J* 5.6, 2H, H9), 3.63 (d, *J* 5.6, 2H, H8), 3.49 (d, *J* 5.6, 2H, H9), 2.91 (t, *J* 8.0, 2H, H6), 2.72 (t, *J* 8.0, 2H, H6), 2.51 (t, *J* 8.0, 2H, H5), 2.30 (t, *J* 8.0, 2H, H5, 2.19 (s, 3H, H4), 1.93 (s, 3H, H4), 1.37 (s, 9H, *t*-butyl), 1.27 (s, 9H, *t*-butyl); δ_c (100 MHz; $CDCl_3$) 151.6, 150.3, 145.6, 136.1, 127.2, 126.4, 125.6, 123.7, 123.6, 122.5, 122.4, 119.0, 98.9, 98.2, 52.7, 52.0, 49.4, 14.2, 49.0, 48.7, 48.5, 47.7, 42.1, 40.8, 32.0, 31.4, 28.4, 22.5, 22.3, 12.6; (Found: *m*/*z* 577.0805 [M+], $C_{31}H_{33}ClN_4O_5$ requires *M*, 577.0798) (Found: C, 66.80, H, 7.39, N, 7.48%; Requires C, 66.95, H, 7.28 N, 7.10%).

2.2. Biological evaluation

2.2.1. Parasite cultivation

D10 and K1 strains of *P. falciparum* were maintained in continuous *in vitro* culture by standard methods [28]. The cultured parasites were, whenever necessary, synchronized by treatment with 5% D-sorbitol (Sigma) at the ring stage [29].

2.2.2. Evaluation of in vitro antiplasmodial activity

The *in vitro* antiplasmodial assays were carried out against D10 and K1 strains of *P. falciparum* using the parasite lactate dehydrogenase assay, as previously reported by Guantai et al. 2010 [30].

2.2.3. Evaluation of β-hematin inhibition

β-hematin inhibition assays were conducted as previously described by Ncokazi *et al.* 2005 [31].

2.2.4. Cytotoxicity assays

Cytotoxicity assays were carried out on a human cervical carcinoma cell line (HeLa) using the MTT [3-(4,5-dimethylthiazol-2-yl)-2,5-diphenyltetrazolium bromide] assay. Briefly, cell cultures were routinely maintained in Eagle's Minimum Essential Medium (EMEM) supplemented with 10% bovine foetal calf serum (FCS). For cytotoxicity evaluations, 5×10^2 cells in 180 μl medium were seeded in each well of a 96-well plate and incubated at 37 °C under a 5% CO_2 atmosphere for 1 h. Aliquots of 20 μl of serial dilutions of the test compounds (stocks in DMSO) were added to

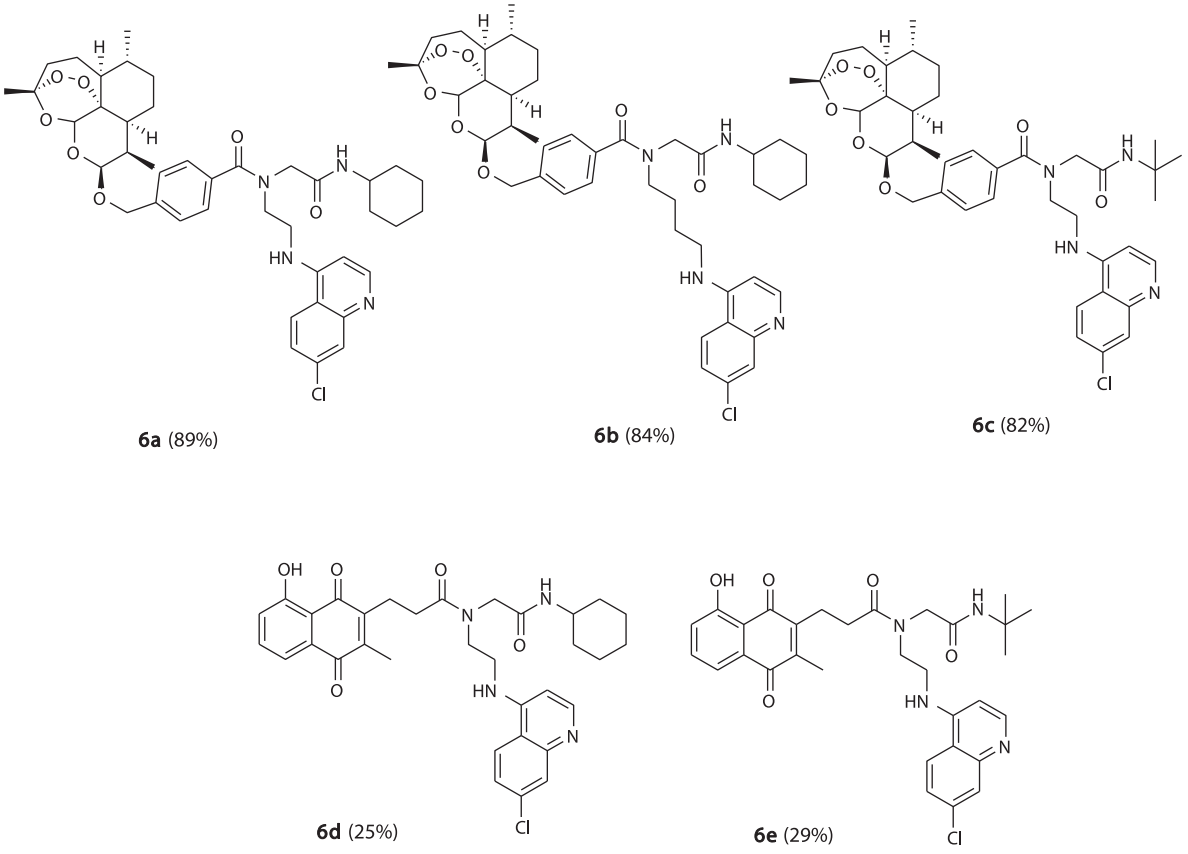

Fig. 3. Target compounds synthesized via the Ugi 4-CC.

the wells. Untreated control wells received 20 μl of culture medium, while additional solvent controls were prepared with medium containing DMSO to account for any possible effects of DMSO on cell viability. The plates were then incubated at 37 °C under an atmosphere of 5% CO_2 for seven days.

After the incubation period, 20 μl MTT (5 mg/ml) was added to each well. The plates were further incubated for an additional 4 h at 37 °C under an atmosphere of 5% CO_2, and then centrifuged for 10 minutes at 800 G. The supernatant was carefully aspirated from each well without disturbing the pellet, and the cells were washed by addition of 150 μl of phosphate-buffered saline (PBS) followed by centrifugation for 10 minutes at 800 G. The supernatant was again carefully aspirated, and the plates were left to dry off at 37 °C for an hour. 100 μl ethanol was added to each well to solubilize the resultant formazan crystals, aided by gentle mechanical shaking for 1–2 h. Absorbances were measured on a Universal Microplate Reader (ELx800 UV, Bio-tek Instruments) at a wavelength of 570 nm and used to calculate percentage cell growth in drug-treated wells; these in turn were plotted versus log drug concentration and used to determine the corresponding IC_{50} values by non-linear regression analysis.

2.2.5. Western blotting and immunofluorescence assays

Western blotting and immunofluorescence assays were conducted as previously reported by Hoppe et al. [24]. Briefly, trophozoite-stage D10 *P. falciparum* parasites were respectively incubated with chloroquine, artesunate and the hybrid compounds for 8 h at five times the IC_{50} of the relevant compounds, released from the red blood cells by saponin treatment and washed extensively to remove extraneous hemoglobin.

Hemoglobin levels in the released parasites were determined by sodium dodecyl sulfate-polyacrylamide gel electrophoresis (SDS-PAGE) and Western blotting with anti-hemoglobin antiserum. To ensure that the different intensities of the hemoglobin bands on the resultant blots were not the result of uneven loading of parasite pellets, gels were also stained with Coomassie dye to visualize protein bands in the gels. No variations in the intensities of the major non-globin proteins were observed in the different samples. Net hemoglobin band intensities on the blots were determined with Kodak 1D image analysis software (version 3.5).

For the immunofluorescence assays, the drug-treated saponin-released parasites were fixed onto poly-lysine-coated glass cover slips with paraformaldehyde-glutaraldehyde, after which they were treated with Triton to enhance their permeability. Parasite-associated hemoglobin was labelled by incubation with anti-Hb antiserum and tetramethylrhodamine-5-isothiocyanate (TRITC)-conjugated secondary antibodies. The cover slips were viewed by fluorescence microscopy and images captured with a CoolSNAP-Pro CCD camera.

3. Results and discussion

3.1. Antiplasmodial activity and cytotoxicity

Antiplasmodial activity against the chloroquine sensitive (CQS) D10 strain and chloroquine resistant (CQR) K1 strain of *P. falciparum*, as well as cytotoxicity against a human cervical cancer cell line (HeLa), were determined for the target compounds and are tabulated in Table 1. Therapeutic indices were calculated by dividing the IC_{50} obtained for HeLa cells with those obtained for the K1 parasite strain. Chloroquine was used as the control for both antiplasmodial and cytotoxicity assays.

The three Ugi adducts containing the artemisinin core (**6a**–**c**) displayed excellent *in vitro* antiplasmodial activities that were

Table 1
Results obtained from the *in vitro* biological evaluation of the intermediates and target compounds for antiplasmodial, anticancer and β-Hematin inhibition activity.

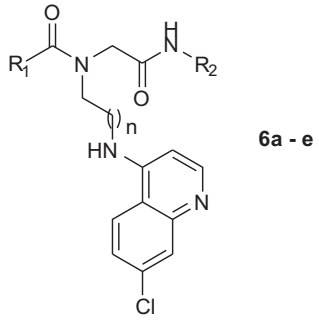

6a - e

.

Cpd	R_1	R_2	*n*	D10 IC_{50} (±SD[a]) μM	K1 IC_{50} (±SD[a]) μM	RI[b]	HeLa IC_{50} (μM)	TI[c]	β-Hematin Inhibition IC_{50} (equiv.)
2	–	–	–	0.006	0.006	1	ND[f]	–	ND[f]
3	–	–	–	38.35 ± 5.085	20.29 ± 4.137	0.53	ND[f]	–	ND[f]
4	–	–	–	1.37	2.56	1.87	ND[f]	–	ND[f]
5	–	–	–	2.15	2.74	1.27	ND[f]	–	ND[f]
6a	ART[d]	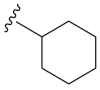	1	0.026 ± 0.0014	0.023 ± 0.0014	0.88	0.286	12	0.45 ± 0.04
6b	ART[d]	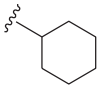	3	0.035 ± 0.0014	0.021 ± 0.0014	0.60	0.169	8	0.31 ± 0.01
6c	ART[d]		1	0.027 ± 0.0015	0.019 ± 0.0015	0.70	0.496	26	0.44 ± 0.04
6c-citrate	ART[d]		1	0.024 ± 0.0012	0.018 ± 0.0012	0.75	0.356	20	0.40 ± 0.01
6d	NQ[e]	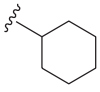	1	0.638 ± 0.0018	0.467 ± 0.0018	0.73	5.211	11	Not active[g]
6e	NQ[e]		1	0.569 ± 0.0019	0.454 ± 0.0020	0.80	6.259	14	Not active[g]
Chloroquine	–	–	–	0.020 ± 0.0033	0.219 ± 0.0023	11	8.54	39	1.91 ± 0.3
Artemisinin	–	–	–	0.023 ± 0.0040	0.014 ± 0.0037	0.61	ND[f]	–	0.66 ± 0.1
DHA	–	ND[f]	–	0.004	0.003	0.75	ND[f]	–	ND[f]

[a] SD = standard deviation of the mean of three independent determinations.
[b] RI, resistance index, calculated as [IC_{50} (K1)]/[IC_{50} (D10)].
[c] TI, therapeutic index, calculated as [IC_{50} (HeLa)]/[IC_{50} (K1)].
[d] ART, artelinic acid core.
[e] NQ, naphthoquinone core.
[f] ND, not determined.
[g] Not active, $IC_{50} > 10.0$ eq.

comparable to chloroquine's activity against the CQS D10 strain (26, 35 and 27 nM for **6a**, **6b** and **6c** respectively, compared with 20 nM for CQ). The salt derivative **6c-citrate** did not exhibit a significant enhancement of *in vitro* activity relative to **6c**. There was no evidence of these artemisinin–chloroquinoline hybrids exhibiting cross-resistance with chloroquine, as shown by the low resistance index (RI) values for this set of compounds relative to chloroquine [RI was calculated by dividing the IC_{50} obtained for the CQR strain (K1) by that of the CQS strain (D10)]. The 1,4-naphthoquinone-chloroquinoline hybrid molecules **6d** and **6e** only exhibited moderate antiplasmodial activities relative to the artemisinin-based hybrids, with IC_{50} values >0.4 μM against both

strains of the malaria parasite. Notably however, they also displayed no evidence of cross-resistance with chloroquine and had low RI values of <1.

The results from the cytotoxicity assay suggest that the hybrid molecules possess moderate selectivity for the malaria parasite relative to mammalian cells. None of the compounds matched the selectivity of chloroquine, which had a calculated therapeutic index (TI) of 39.

3.2. β-Hematin Inhibition

The hybrid compounds were tested for their ability to inhibit the crystallization of hematin to β-hematin *in vitro* using a colorimetric β-hematin inhibition screening assay [31], and the results are also tabulated in Table 1.

Chloroquine was used as the control, and had an IC_{50} value of 1.91 eq. All three hybrid molecules that contain the artemisinin core displayed enhanced β-hematin inhibitory activity when compared to chloroquine and artemisinin, with IC_{50} values of 0.45, 0.31 and 0.44 eq for **6a**, **6b** and **6c**, respectively. The salt derivative **6c-citrate** displayed activity similar to the free base **6c**. Compounds **6d** and **6e**, which contain the 1,4-naphthoquinone core, displayed no inhibitory activity at the highest concentration tested (10 eq). This suggested that the presence of the 1,4-naphthoquinone moiety may interfere with the β-hematin inhibitory mechanism of the 4-aminoquinoline pharmacophore, and probably explains why these two compounds exhibited relatively lower *in vitro* antiplasmodial activities. Interestingly, we were surprised to observe that artemisinin inhibited β-hematin formation with a lower IC_{50} value of 0.66 eq in our assay. This observed potency of artemisinin in inhibiting β-hematin formation is quite controversial, especially in light of existing reports suggesting that artemisinin antimalarials do not inhibit β-hematin/hemozoin formation [32].

The controversy surrounding the possible effects of artemisinin antimalarials on hemozoin formation is longstanding, and a look at the literature suggests that the presence or absence of observed effects is highly dependent on the assay applied and the attendant conditions. For example, both quinoline as well as endoperoxide antimalarials showed notable inhibition of β-hematin formation catalyzed by the cell free homogenate of *Plasmodium yoelii* [33,34]; this inhibition was more pronounced in a more sensitive plasma-based assay (pH 4.8), with IC_{50}s of 17.6 μM (CQ), 4.5 μM (artemisinin) and 1.9 μM (α/β arteether) [34]. In related studies, artemisinin and dihydroartemisinin showed a dose-dependent inhibition in the heme polymerization inhibitory activity (HPIA) assay (hematin in acetic acid at pH 3, 37 °C, 24 h), with a mole ratio (dihydroartemisinin:hematin) of 1.61 inhibiting β-hematin polymerization by 50% [35]. In contrast, no inhibition was observed with dihydroartemisinin in a β-hematin inhibitory activity (BHIA) assay (hemin in dimethyl sulfoxide-acetate buffer at pH 5.0, 37 °C, 18 h) [32].

It has been argued that the inhibition of β-hematin formation in the HPIA assay by artemisinin and dihydroartemisinin reflects a reactivity (resulting from axial interactions between the artemisinin and hematin) that is not related to their antimalarial action; the absence of activity in the BHIA assay (which is believed to screen for those molecules forming π–π interactions with hematin and thus inhibiting β-hematin formation) is thought to suggest that these endoperoxide compounds do not exert their antimalarial activity by inhibiting hemozoin formation [32,36]. Interestingly, our results were derived using a standardized BHIA assay (hematin, dimethyl sulfoxide-acetate buffer at pH 5.0, 60 °C, 1 h) as reported by Ncokazi et al. [31], and showed significant inhibition of β-hematin formation by artemisinin; this is despite the similarity in conditions with the previously reported [36] BHIA assay, and further fuels the controversy that still surrounds the effects of artemisinin compounds on β-hematin/hemozoin formation.

Furthermore, in previous work we have found no effect of artesunate on β-hematin formation, so we ourselves were initially very surprised by this result with artemisinin. Nonetheless, repeat experiments gave the same result and forced us to the conclusion that artemisinin does not behave in the same way as artesunate, at least in this assay. The failure to observe inhibition in previous studies may be a result of the reliance on the intrinsic absorbance of soluble hematin, whereas the current assay converts unreacted hematin to a distinct low-spin heme-pyridine complex which can be more reliably measured.

Notwithstanding the above mentioned controversies, all data produced so far by various authors needs to be reviewed in light of the more recent disclosure that beta-hematin formation occurs at the interface of lipid droplet-like structures dubbed lipid nanospheres [37]. The physico-chemical properties of this interface environment differ markedly from bulk aqueous medium and the effects of artemisinins in this milieu remain to be explored. This finding has serious implications on the aforementioned controversy surrounding inhibition of β-hematin formation by the artemisinin class of drugs. On the basis of this more recent finding, the different physico-chemical properties of artemisinin, dihydroartemisin, arteether and artesunate should be factored into any argument. A detailed investigation of the effect on beta-hematin formation at the lipid bilayer interface needs to be conducted for artemisinin, dihydroartemisin, arteether and artesunate.

3.3. Morphological changes in the parasites

In order to monitor for changes in parasite morphology, the artemisinin–chloroquinoline hybrid compounds **6a–c** were added to ring- and trophozoite-stage cultures respectively at concentrations five times their respective IC_{50} values. At appropriate time intervals after addition of the compounds, parasite-infected erythrocytes were smeared onto microscope slides, fixed with methanol and stained with Giemsa before viewing under a light microscope. Microscope images for untreated and drug-treated rings are shown in Fig. 4A. Control (untreated) ring stage parasites were still in the ring stage after 6 h, but had developed into prominent trophozoites after 24 h and 30 h. At 48 h, parasites had progressed through a round of asexual reproduction to produce new rings. When ring-stage parasites were treated with chloroquine, no morphological changes were observable after 6 h. This was expected, as chloroquine has been widely accepted to target parasites at the actively metabolizing trophozoite stage [38,39]. However, 24 and 30 h after drug treatment, the majority of the parasites in the cell culture still remained in the ring stage, as opposed to developing into trophozoites. This suggested that chloroquine action had retarded parasite life-cycle progression. After 48 h, the majority of the parasites had developed into trophozoites with apparently enlarged food vacuoles and had not undergone nuclear division to form schizonts.

Artemisinin appeared to be much faster-acting than chloroquine on ring-stage parasites, as dying parasites could already be observed in the artemisinin-treated culture at 24 h after addition, evidenced by the decrease in size and the contracted, pyknotic appearance of the rings. Smears of the culture at 30 and 48 h indicated that the culture predominantly consisted of non-viable ring remnants, appearing as tiny, dense dots. Non-viable rings in the culture indicate that artemisinin displays marked parasiticidal activity on the ring stage, completely preventing survival and progression into the trophozoite stage. This is consistent with the *in vivo* findings that artemisinins cause a rapid reduction of parasitemia to below detectable levels [40,41].

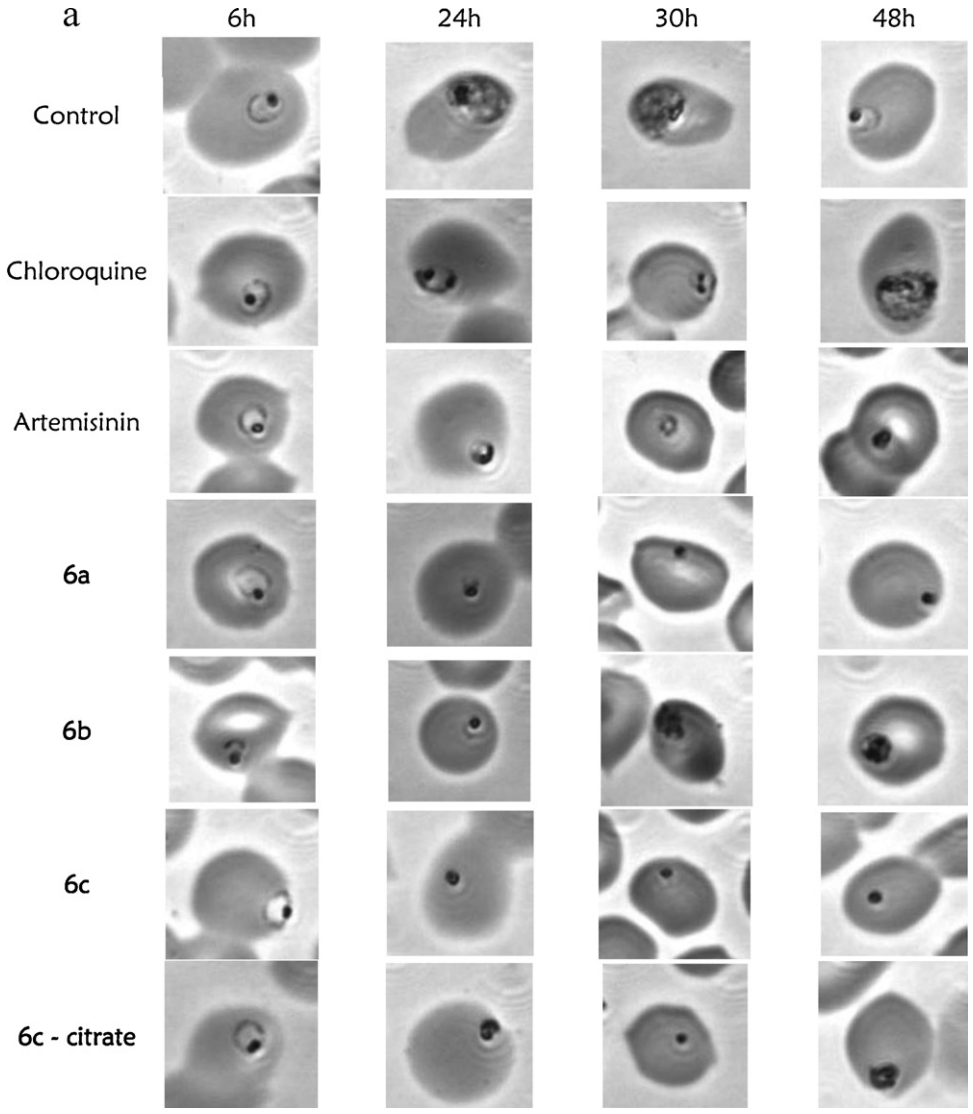

Fig. 4. (A) Light microscopy images of Giemsa-stained parasites at various time-points after the addition of drugs to ring stage parasites. (B) Light microscopy images of Giemsa-stained parasites at various time-points after addition of drugs to trophozoite stage parasites.

Morphological changes in the ring-stage parasites treated with hybrid molecules **6a–c** and its salt all followed the same pattern as that of artemisinin, with cultures mainly consisting of non-viable rings by 24 h after drug addition. In the culture treated with compound **6b**, a small percentage of abnormal and pyknotic early trophozoites were also observed at 30 and 48 h after drug addition.

In a second set of morphology experiments, compounds were added to parasites in the trophozoite stage and incubated for 48 h. Light microscope images of untreated and drug-treated trophozoites are shown in Fig. 4B. After 6 h, the control (untreated) trophozoites started undergoing nuclear division (the multiple nuclei produce a marked punctate appearance in the parasite cytoplasm) to become schizonts. These daughter nuclei in the schizont develop into small, invasive merozoites, and at 24 h and 30 h these merozoites were observed to have invaded fresh red blood cells and developed into rings which further developed into trophozoites that predominated at 48 h.

Effects of chloroquine treatment on trophozoites were much more pronounced than on the ring stage. Morphological changes after 6 h demonstrated that chloroquine had already exerted considerable effects on these parasites as the trophozoites were observed to be smaller and denser, a clear indication of stress on the parasites. After 24 h of drug treatment, deformed schizonts with few nuclei were observed, and this unusual morphology was maintained for a further 24 h. Morphological changes in artemisinin-treated parasites were somewhat different to those incubated with chloroquine. After 6 h, parasites seemed to be initiating nuclear division and entering the schizont stage, though they did not appear to progress further than this as the parasites were still predominantly in this stage up to 24 h after artemisinin treatment. At 30 and 48 h after drug treatment, pyknotic, darkly stained parasite remnants were mostly observed.

The artemisinin-based hybrid compounds **6a–c** appeared to act faster than chloroquine or artemisinin; a small percentage of the parasites had already taken on the contracted appearance of dying parasites after just 6 h of drug exposure, and after 24 h of drug treatment most of the parasites appeared non-viable.

From the study of morphological changes of the drug-treated parasites, it was evident that chloroquine's parasiticidal action is mainly directed against trophozoite stage parasites, while its effect on ring stage parasites is to slow/disrupt development into trophozoites. By marked contrast, artemisinin is parasiticidal

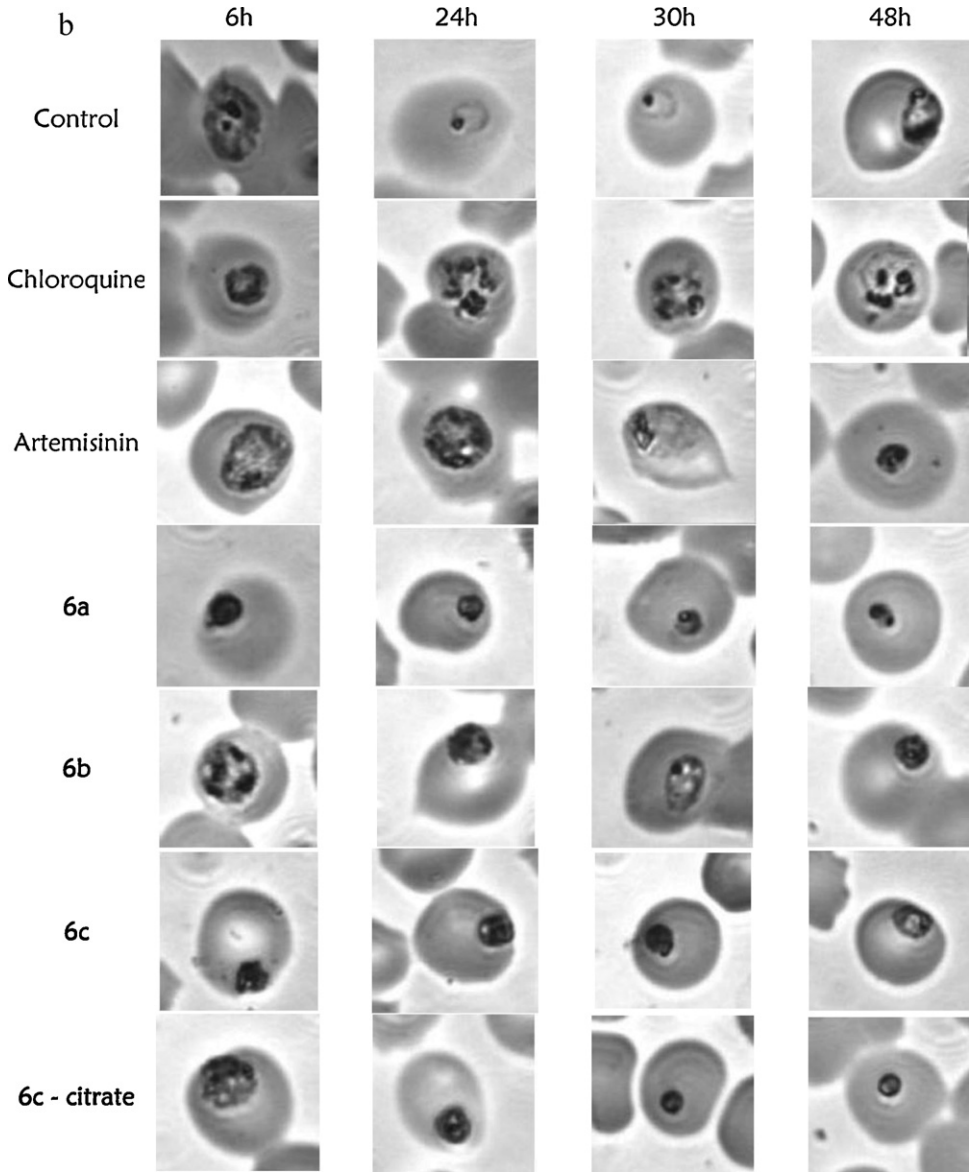

Fig. 4. (*Continued*).

against all stages of parasites and has a more rapid action. These findings corresponded to findings published in literature [38,39,42,43]. Importantly, the blood smears of cultures treated with the hybrid molecules indicate that these compounds shared the rapid parasiticidal action and broad stage-specificity of artemisinin, and produced similar morphological changes.

3.4. Effect on endocytosis: hemoglobin levels

It has previously been shown that chloroquine blocks hemoglobin degradation and causes an increase in parasite-associated hemoglobin [44,45]. Based on their pronounced antiplasmodial activities (Table 1), compounds **6a–c** and its salt were investigated by Western blotting for their effects on hemoglobin levels in the parasites and compared to chloroquine and artesunate.

It was evident from the Western blots (Fig. 5) that both chloroquine and artesunate treatment caused an increase in hemoglobin level in the parasites relative to the untreated controls,

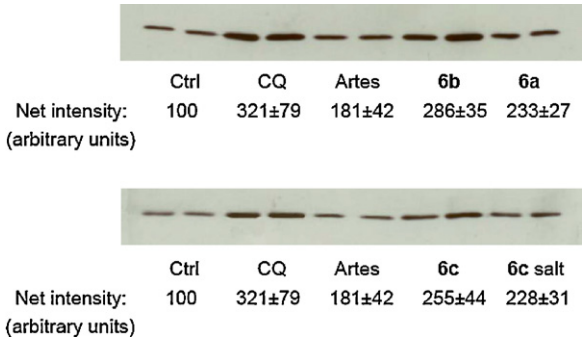

Fig. 5. Western blots of hemoglobin levels in parasites. Parasites were left untreated (ctrl), or incubated with chloroquine (CQ), artesunate (Artes), or hybrid compounds **6a–c** and its salt at 37 °C for 5 h. Net intensities of individual bands were determined with Kodak 1D image analysis software, version 3.5. Normalized values ± SD obtained from five independent experiments are shown.

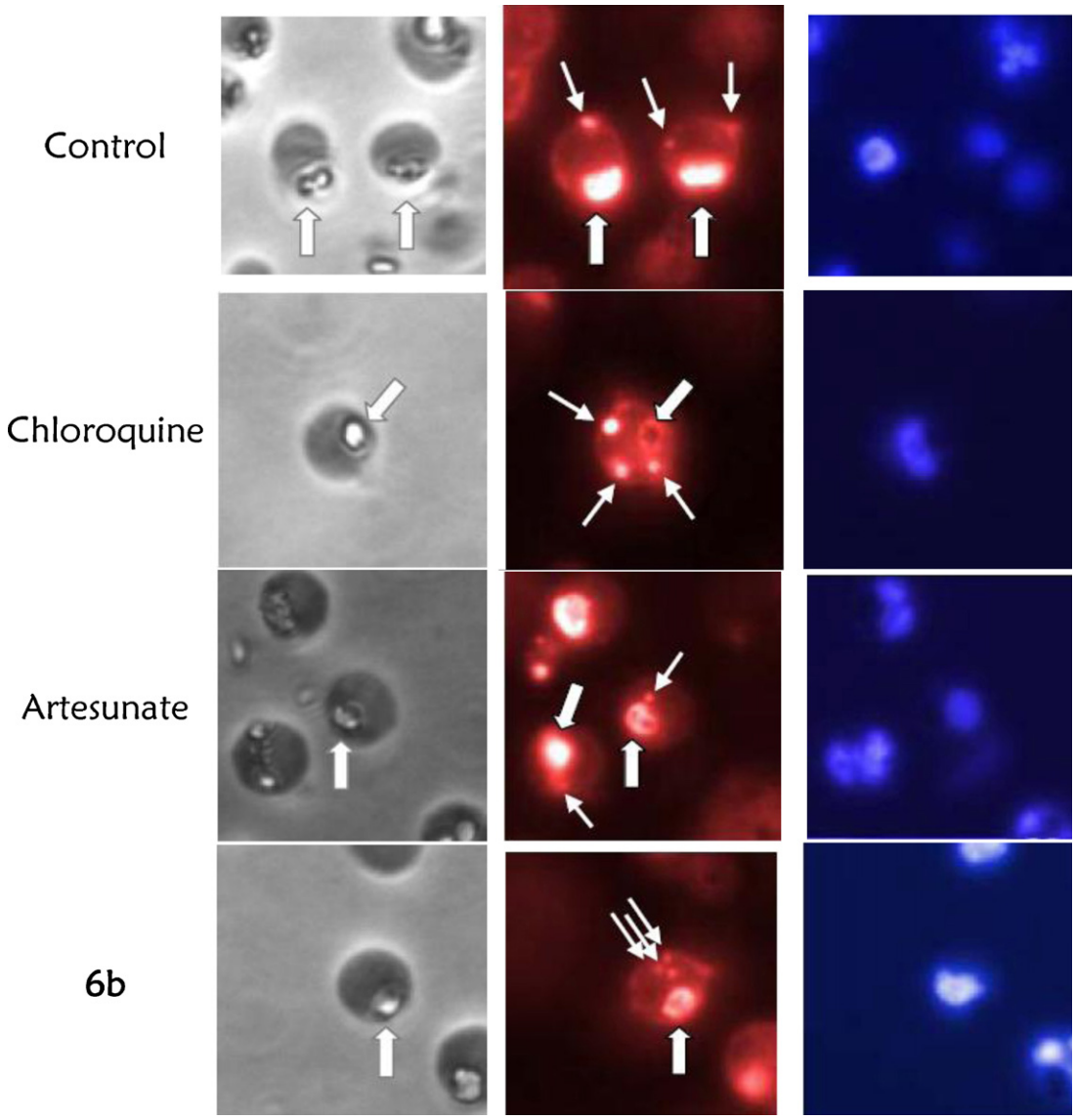

Fig. 6. Immunofluorescence microscopy localization of hemoglobin in parasites following incubation with various drugs. The position of the food vacuole (FV) is indicated by large arrows, whereas those of the hemoglobin-containing transport vesicles are indicated by small arrows. Control: untreated parasites; Phase: phase-contrast images, Hb: localization of hemoglobin; DAPI: nucleic acids were stained using DAPI in order to determine the number of nuclei, to avoid including multi-nucleated schizonts in the analyses.

although the increase associated with artesunate was considerably less than that obtained with chloroquine. These results are in agreement with published results [24,46]. The hybrid molecules also produced an increase in parasite hemoglobin levels compared to the controls, and these effects were intermediate between those observed for chloroquine and artesunate.

3.5. Effect on endocytosis: localization of transport vesicles by immunofluorescence microscopy

To further investigate the effects of the artemisinin–chloroquinoline hybrid molecules on the endocytic pathway, the subcellular location of hemoglobin within parasites after drug exposure was determined by immunofluorescence microscopy using anti-hemoglobin antiserum. Compound **6b** was selected for the immunofluorescence assay from among the hybrid species as it showed the most significant increase in hemoglobin as detected by Western blotting.

Parasite-associated hemoglobin is predominantly located in the food vacuole. Ultra-structural studies have suggested that the increase in hemoglobin level in chloroquine-treated parasites may be due to the presence of endocytic vesicles (or hemoglobin transport vesicles) filled with undigested hemoglobin found either in the food vacuole [47] or throughout the parasite cytoplasm [24]. To investigate the effects of the target compounds on endocytic trafficking within the parasite, subcellular localization of hemoglobin was visualized by immunofluorescence microscopy, with particular emphasis on the amount of hemoglobin in the food vacuole and the numbers and distribution of endocytic vesicles. Representative images are shown in Fig. 6.

In the control parasites, hemoglobin was predominantly located in the food vacuole (FV). The location of the FV is readily determined by referring to the corresponding phase-contrast images, where the shiny hemozoin crystals, formed from hemoglobin degradation in the FV are prominently visible. The food vacuoles are further indicated by large arrows in the

fluorescence images. Punctate endocytic vesicles, filled with hemoglobin, were also visible. These are indicated by small arrows.

For chloroquine treated parasites, there was little fluorescence (or in some cases, no fluorescence) in the FV, and hemoglobin was mostly found enclosed in endocytic vesicles. Treatment with artesunate and **6b** resulted in fewer endocytic vesicles when compared to control parasites. The average number of transport vesicles per parasite was enumerated by counting the amount of visible vesicles (appearing as fluorescent foci separate from the food vacuole) in 100–400 parasites per treatment. It was found that the average number of transport vesicles increased significantly in chloroquine-treated parasites (4.5) relative to the untreated parasites (1.54), but decreased in parasites treated with artesunate and **6b** (0.89 and 0.91, respectively).

The results obtained for chloroquine and artesunate agreed with those reported in literature. As discussed above, Hoppe et al. [24] suggested that the increase in hemoglobin accumulation and the number of transport vesicles in chloroquine-treated parasites may be the result of a block in transport vesicle-vacuole fusion, which reduces the delivery of hemoglobin to the food vacuole for digestion. In addition, the decrease in endocytic vesicle counts in artesunate-treated parasites agrees with the reported inhibition of endocytosis by this drug – decreased hemoglobin endocytosis should decrease the rate of endocytic vesicle formation and hence lower the vesicle content per parasite. Crespo et al. [48] also report that ring-stage parasite-infected erythrocytes treated for 24 h with artemisinin at two times its IC_{50} value advanced to the trophozoite stage but showed a marked loss of organellar structures accompanied by the disintegration of many of the major membrane-bound features.

At concentrations much higher than those applied in this study, artemisinin-treatment has been reported to result in loss of digestive vacuole integrity in trophozoite-infected erythrocytes treated for 4 h. After 8 h of treatment with the endoperoxide antimalarials, more dramatic effects on parasite morphology were observed, including the disruption of the digestive vacuole membrane and the release of hemozoin crystals into the parasite cytoplasm. [48].

The morphology and immunofluorescence assays suggest that the mode of action of the hybrid molecules more closely resembles that of the artemisinin parent drug rather than that of chloroquine. The hybrid molecules and artemisinin rapidly kill parasites in the ring stage, as opposed to the parasiticidal action of chloroquine which is more prolonged and prevalent in the trophozoite stage. In addition, the hybrid molecules and artemisinin reduced the amount of hemoglobin-filled endocytic vesicles in the parasite, likely due to an inhibition of endocytosis, in contrast to the vesicle-vacuole fusion block and marked increase in vesicles caused by chloroquine. The fact that the increase in overall hemoglobin levels in the parasite obtained with the hybrids, as judged by Western blotting, is intermediate between the increase observed with artesunate and chloroquine respectively suggests that an element of chloroquine's mode of action may be maintained in the hybrid molecules.

The moderate increase in overall parasite hemoglobin levels caused by artemisinin has been interpreted as a combination of decreased hemoglobin uptake due to a block in endocytosis on the one hand, balanced by increased hemoglobin content due to an inhibition of hemoglobin proteolysis in the food vacuole on the other [24]. The β-hematin inhibition assays suggest that the hybrid compounds could be even more effective than chloroquine at inhibiting the formation of hemozoin crystals in the food vacuole. Vacuole damage caused by heme accumulation may result in more extensive hemoglobin proteolysis inhibition by the hybrids than with the artemisinin parent drug, thus explaining the greater extent of hemoglobin accumulation observed by Western blotting.

In conclusion, 4-Aminoquinolines were hybridized with artemisinin and 1,4-naphthoquinone derivatives via the Ugi-4CC reaction and their biological activities were investigated. No cross-resistance with chloroquine was observed for these hybrid compounds in chloroquine resistant malaria parasites, despite the fact that they contained the chloroquinoline moiety. The artemisinin-containing compounds **6a–c** and its salt were the most active target compounds in the antiplasmodial assays. They were also potent inhibitors of β-hematin formation. However, despite the potent *in vitro* activities, they also displayed notable cytotoxicity and had lower therapeutic indices than chloroquine. Morphological changes in parasites treated with compounds **6a–c** and its salt have shown that they may act by mechanism(s) similar to artemisinin, as both ring and trophozoite stage parasites were affected by the drug treatment. Additionally, the potent β-hematin inhibitory activities of these hybrids may contribute to their inhibitory mechanism(s) against trophozoite stage parasites. The effects of the artemisinin-containing hybrids on endocytosis were also investigated, and were found to result in an increase in accumulation of hemoglobin within the parasites. Subsequent immunofluorescence studies showed that, for the representative compound **6b**, there was a decrease in the number of transport vesicles in the parasites. These hybrid molecules may therefore act by inhibition of endocytosis, as suggested by the immunofluorescence results, as well as by inhibition of hemoglobin degradation, as suggested by the observed increase in hemoglobin levels in the parasites seen on the Western blots.

The morphological study reported here constituted a qualitative assessment of the stage-specificity and rate of action of the active hybrid compounds *vis-a-vis* chloroquine and artemisinin. The results suggested a more artemisinin-like action for the hybrid compounds. Attempts were not made to accurately quantify the morphological changes, given the intrinsic difficulties in confidently categorising the morphological state of each individual parasite by light microscopy, caused by the heterogeneity and graded nature of morphological responses of individual cells to the drug interventions (unless the changes are drastic, uniform and advanced). It is due to the inherent qualitative nature of the morphological evaluations that additional independent and more quantifiable read-outs of chloroquine and artemisinin action were sought - in this case measuring hemoglobin levels and transport vesicle numbers in treated parasites. The results from the latter experiments agree with the morphological study in suggesting a more artemisinin-like action for the hybrid compounds.

An obvious limitation to this work presented here, and which is a universal limitation when evaluating the cell biological consequences of antimalarial drug treatment, is difficulty in distinguishing between "effects that are the result of a primary mechanism of action of the drug (e.g., a direct interaction of the drugs or their adducts with the endocytosis or fusion machinery of the cell), an important secondary effect of a more general perturbation (e.g., pH changes or membrane damage), or a nonspecific manifestation of a cell that is stressed and dying" [24].

Acknowledgments

Financial support from the following sources is gratefully acknowledged: the South African National Research Foundation (T-SF, EMG, TJE); the South African Research Chairs Initiative (SARChI) of the Department of Science and Technology (DST) administered through the South African National Research Foundation (KC); the South African Medical Research Council (MRC) and the University of Cape Town (KC, TJE); the Cancer Association of South Africa (CANSA) (KC); and the Welcome Trust through a Senior International Research Fellowship (HH).

References

[1] Thwing J, Skarbinski J, Newman RD, Barber AM, Mali S, Roberts JM, et al. Malaria Surveillance—United States, 2005. Surveil Summ 2007;56:23–8.
[2] WHO. World malaria report; 2008.
[3] WHO Expert Committee on Malaria. WHO technical report series twentieth report; 2000.
[4] Kumar A, Katiyar SB, Agarwal A, Chauhan PMS. Perspective in antimalarial chemotherapy. Curr Med Chem 2003;10:1137–50.
[5] Price RN, Nosten F. Drug resistant falciparum malaria: clinical consequences and strategies for prevention. Drug Resist Update 2001;4:187–96.
[6] WHO. Guidelines for the treatment of malaria. WHO; 2006.
[7] Noedl H, Se Y, Schaener K, Smith BL, Socheat D, Fukuda MM. Evidence of artemisinin-resistant malaria in Western Cambodia. N Engl J Med 2008;359:2619–20.
[8] Dondorp AM, Norsten F, Yi P, Das D, Phyo AP, Tarning J, et al. Artemisinin resistance in *Plasmodium falciparum* malaria. N Engl J Med 2009;361:455–67.
[9] Ridley RG, Medical need. scientific opportunity and the drive for antimalarial drugs. Nature 2002;415:686–93.
[10] Coatney GR. Pitfalls in a discovery: the chronicle of chloroquine. Am J Trop Med Hyg 1963;12:121–8.
[11] Haynes RK. From artemisinin to new artemisinin antimalarials: biosynthesis, extraction, old and new derivatives, stereochemistry and medicinal chemistry requirements. Curr Top Med Chem 2006;6:509–37.
[12] Woodrow CJ, Haynes RK, Krishna S. Artemisinins. Postgrad Med J 2005;81:71–8.
[13] Jones M, Mercer AE, Stocks PA, la Pensee LJI, Cosstick R, Park BK, Kennedy ME, Piantanida I, Ward SA, Davies J, Bray PG, Rawe SL, Baird J, Charidza T, Janneh O, O'Neill PM. Antitumour and antimalarial activity of artemisinin-acridine hybrids. Bioorg Med Chem Lett 2009;19:2033–7.
[14] Araujo NCP, Barton V, Jones M, Stocks PA, Ward SA, Davies J, Bray PG, Shone AE, Cristiano MLS, O'Neill PM. Semi-synthetic and synthetic 1,2,4-trioxaquines and 1,2,4-trioxolaquines: synthesis, preliminary SAR and comparison with acridine endoperoxide conjugates. Bioorg Med Chem Lett 2009;19:2038–43.
[15] Biot C, Bauer H, Schirmer RH, Davioud-Charvet E. 5-Substituted tetrazoles as bioisosteres of carboxylic acids. bioisosterism and mechanistic studies on glutathione reductase inhibitors as antimalarials. J Med Chem 2004;47:5972–83.
[16] Davioud-Charvet E, Delarue S, Biot C, Schwöbel B, Boehme CC, Müssigbrodt A, et al. A prodrug form of a *Plasmodium falciparum* glutathione reductase inhibitor conjugated with a 4-anilinoquinoline. J Med Chem 2001;44:4268–76.
[17] Atamna H, Ginsburg H. Heme degradation in the presence of glutathione. J Biol Chem 1995;270:24876–83.
[18] Weissbuch I, Leiserowitz L. Interplay between malaria, crystalline hemozoin formation, and antimalarial drug action and design. Chem Rev 2008;108:4899–914.
[19] Egan TJ, Combrinck JM, Egan J, Hearne GR, Marques HM, Ntenteni S, et al. Fate of haem iron in the malaria parasite *Plasmodium falciparum*. Biochem J 2002;365:343–7.
[20] Friebolin W, Jannack B, Wenzel N, Furrer J, Oeser T, Sanchez CP, et al. Antimalarial dual drugs based on potent inhibitors of glutathione reductase from *Plasmodium falciparum*. J Med Chem 2008;51:1260–77.
[21] Chavain N, Davioud-Charvet E, Trivelli X, Mbeki L, Rottmann M, Brun R, et al. Antimalarial activities of ferroquine conjugates with either glutathione reductase inhibitors or glutathione depletors via a hydrolyzable amide linker. Bioorg Med Chem 2009;17:8048–59.
[22] Ugi I, Steinbrückner C. On a new condensation principle. Angew Chem 1960;72:267–8.
[23] Dömling A, Ugi I. Multicomponent Reactions with Isocyanides. Angew Chem Int Ed 2000;39:3168–210.
[24] Hoppe HC, van Schalkwyk DA, Wiehart UIM, Meredith SA, Egan J, Weber BW. Antimalarial quinolines and artemisinin inhibit endocytosis in *Plasmodium falciparum*. Antimicrob Agents Chemother 2004;48:2370–8.
[25] Lin AJ, Klayman DL, Milhous WK. Antimalarial activity of new water-soluble dihydroartemisinin derivatives. J Med Chem 1987;30:2147–50.
[26] Salmon-Chemin L, Bruisine E, Yardley V, Kohler S, Debreu M-A, Landry V, et al. 2- and 3-Substituted 1,4-naphthoquinone derivatives as subversive substrates of trypanothione reductase and lipoamide dehydrogenase from *Trypanosoma cruzi*: synthesis and correlation between redox cycling activities and *in vitro* cytotoxicity. J Med Chem 2001;44:548–65.
[27] Peck RM, Preston RK, Creech HJ. Nitrogen mustard analogs of antimalarial drugs. J Am Chem Soc 1959;81:3984–9.
[28] Trager W, Jensen JB. Human malaria parasites in continuous culture. Science 1976;193:673–5.
[29] Lambros C, Vanderberg JP. Synchronization of *Plasmodium falciparum* erythrocyte stages in culture. J Parasitol 1979;65:418–20.
[30] Guantai EM, Smith PJ, Gut J, Rosenthal PJ, Chibale K. Design, synthesis and *in vitro* antimalarial evaluation of triazole-linked chalcone and dienone hybrid compounds. Bioorg Med Chem 2010;18:8243–56.
[31] Ncokazi K, Egan T. A colorimetric high-throughput β-hematin inhibition screening assay for use in the search for antimalarial compounds. Anal Biochem 2004;338:306–19.
[32] Haynes RK, Monti D, Taramelli D, Basilico N, Parapini S, Olliaro P. Artemisinin antimalarials do not inhibit hemozoin formation. Antimicrob Agents Chemother 2003;47:1175.
[33] Pandey AV, Tekwani BL, Singh RL, Chauhan VS. Artemisinin, an endoperoxide antimalarial, disrupts the hemoglobin catabolism and heme detoxification systems in malarial parasite. J Biol Chem 1999;274:19383–8.
[34] Tripathi AK, Gupta A, Garg SK, Tekwani B. *In vitro* β-hematin formation assays with plasma of mice infected with Plasmodium yoelii and other parasite preparations: comparative inhibition with quinoline and endoperoxide antimalarials. Life Sci 2001;69:2725–33.
[35] Basilico N, Pagani E, Monti D, Olliaro P, Taramelli D. A microtitre-based method for measuring the haem polymerization inhibitory activity (HPIA) of antimalarial drugs. J Antimicrob Chemother 1998;42:55–60.
[36] Parapini S, Basilico N, Pasini E, Egan TJ, Olliaro P, Taramelli D, et al. Standardization of the physicochemical parameters to assess *in vitro* the β-hematin inhibitory activity of antimalarial drugs. Exp Parasitol 2000;96:249–56.
[37] Pisciotta JM, Coppens I, Tripathi AK, Scholl PF, Shuman J, Bajad S, et al. The role of neutral lipid nanospheres in *Plasmodium falciparum* haem crystallization. Biochem J 2007;402:197–204.
[38] Yayon A, van de Waa JA, Yayon M, Geary TG, Jensen JB. Stage-dependent effects of chloroquine on *Plasmodium falciparum in vitro*. J Euk Microbiol 1983;30:642–7.
[39] Terkuile F, White NJ, Holloway P, Pasvol G, Krishna S. *Plasmodium falciparum*: *in vitro* studies of the pharmacodynamic properties of drugs used for the treatment of severe malaria. Exp Parasitol 1993;76:85–95.
[40] Björkman A, Bhattarai A. Public health impact of drug resistant *Plasmodium falciparum* malaria. Acta Trop 2005;94:163–9.
[41] Krishna S, Uhlemann A-C, Haynes RK. Artemisinins: mechanisms of action and potential for resistance. Drug Resist Update 2004;7:233–44.
[42] Meshnick SR, Artemisinin:. mechanisms of action, resistance and toxicity. Int J Parasitol 2002;32:1655–60.
[43] Meshnick SR. Artemisinin antimalarials: mechanism of action and resistance. Med Trop Mars 1998;58:13–7.
[44] Famin O, Ginsburg H. Differential effects of 4-aminoquinoline-containing antimalarial drugs on hemoglobin digestion in *Plasmodium falciparum*-infected erythrocytes. Biochem Pharmacol 2002;63:393–8.
[45] Zhang Y. Inhibition of hemoglobin degradation in *Plasmodium falciparum* by chloroquine and ammonium chloride. Exp Parasitol 1987;64:322–7.
[46] Roberts L, Egan TJ, Joiner KA, Hoppe HC. Differential effects of quinoline antimalarials on endocytosis in *Plasmodium falciparum*. Antimicrob Agents Chemother 2008;52:1840–2.
[47] Yayon A, Timberg R, Friedman S, Ginsburg H. Effects of chloroquine on the feeding mechanism of the intraerythrocytic human malarial parasite *Plasmodium falciparum*. J Euk Microbiol 1984;31:367–72.
[48] Crespo MP, Avery TD, Hanssen E, Fox E, Robinson TV, Valente P, et al. Artemisinin and a series of novel endoperoxide antimalarials exert early effects on digestive vacuole morphology. Antimicrob Agents Chemother 2008;52:98–109.